

Therapeutic effects of in vivo administration of an inhibitor of tryptophan 2,3-dioxygenase (680c91) for the treatment of fibroids: a preclinical study

Tsai-Der Chuang, Ph.D.,^{a,b} Nhu Ton, B.S.,^b Shawn Rysling, B.S.,^b Derek Quintanilla, B.S.,^b Drake Boos, B.S.,^b and Omid Khorram, M.D., Ph.D.^{a,b,c}

^a Department of Obstetrics and Gynecology, Harbor-UCLA Medical Center, Torrance, California; ^b The Lundquist Institute for Biomedical Innovation, Torrance, California; and ^c Department of Obstetrics and Gynecology, David Geffen School of Medicine at University of California, Los Angeles, Los Angeles, California

Objective: Fibroids are characterized by marked overexpression of tryptophan 2,3 dioxygenase (TDO2). The objective of this study was to determine the effectiveness of in vivo administration of an inhibitor of TDO2 (680C91) on fibroid size and gene expression.

Design: Animal and ex vivo human study.

Setting: Academic Research Institution.

Subjects: Severe combined immunodeficiency mice bearing human fibroid xenografts treated with vehicle and TDO2 inhibitor.

Intervention: Daily intraperitoneal administration of 680C91 or vehicle for 2 months and in vitro studies with fibroid explants.

Main Outcome Measures: Tumor weight and gene expression profile of xenografts and in vitro mechanistic experiments using fibroid explants.

Results: Compound 680C91 was well-tolerated with no effects on blood chemistry and body weight. Treatment of mice with 680C91 resulted in 30% reduction in the weight of fibroid xenografts after 2 months of treatment and as expected lower levels of kynurenine, the byproduct of tryptophan degradation and an endogenous ligand of aryl hydrocarbon receptor (AhR) in the xenografts. The expression of cytochrome P450 family 1 subfamily B member 1 (CYP1B1), transforming growth factor β 3 (TGF- β 3), fibronectin (FN1), cyclin-dependent kinase 2 (CDK2), E2F transcription factor 1 (E2F1), interleukin 8 (IL-8) and secreted protein acidic and cysteine rich (SPARC) mRNA were lower in the xenografts of mice treated with 680C91 compared with vehicle controls. Similarly, the protein abundance of collagen, FN1, CYP1B1, and SPARC were lower in the xenografts of 680C91-treated mice compared with vehicle controls. Immunohistochemical analysis of xenografts indicated decreased expression of collagen, Ki67 and E2F1 but no significant changes in cleaved caspase 3 expression in mice treated with 680C91. The levels of kynurenine in the xenografts showed a direct correlation with the tumor weight and FN1 levels. In vitro studies with fibroid explants showed a significant induction of CYP1B1, TGF- β 3, FN1, CDK2, E2F1, IL8, and SPARC mRNA by tryptophan, which could be blocked by cotreatment with 680C91 and the AhR antagonist CH-223191.

Conclusion: The results indicate that correction of aberrant tryptophan catabolism in fibroids could be an effective treatment through its effect to reduce cell proliferation and extracellular matrix accumulation. (Fertil Steril® 2024;121:669-78. ©2023 by American Society for Reproductive Medicine.)

El resumen está disponible en Español al final del artículo.

Key Words: Fibroid, tryptophan, aryl hydrocarbon receptor, TDO2, xenograft

Received September 6, 2023; revised November 16, 2023; accepted December 4, 2023; published online December 10, 2023.

Supported by National Institutes of Health (NIH); [HD100529, HD100529-0251, HD101852 and HD109286].

Correspondence: Omid Khorram, M.D., Ph.D., Department of Obstetrics and Gynecology, Harbor-UCLA Medical Center, Box 467, 1102 W. Carson St., Torrance, California 90502 (E-mail: okhorram@lundquist.org).

Fertility and Sterility® Vol. 121, No. 4, April 2024 0015-0282/\$36.00

Copyright ©2023 American Society for Reproductive Medicine, Published by Elsevier Inc.

<https://doi.org/10.1016/j.fertnstert.2023.12.006>

Uterine fibroids are common benign uterine smooth muscle tumors, affecting up to 40%–70% of reproductive-aged women (1–3). These tumors can cause abdominal and pelvic pain, excessive menstrual bleeding, and infertility (1–3). The mechanism underlying the pathogenesis of fibroids is not fully understood and the subject of intense investigation. Recently, our group reported for the first time a marked dysregulation of tryptophan degradation pathway with marked overexpression of tryptophan 2,3 dioxygenase (TDO2) and indoleamine 2,3-dioxygenase 1 (IDO1) mRNA and protein in fibroids compared with their matched myometrium (4, 5). These enzymes catalyze the first step in the degradation of tryptophan to N-formylkynurenine, which then is hydrolyzed to kynurenine by N-formyl-L-kynurenine formamidase (6). The levels of kynurenine are a reflection of TDO2/IDO1 enzyme activity and as would be expected we showed fibroids had higher kynurenine levels compared with myometrium (4, 5). We also found that race and the presence of Mediator Complex Subunit 12 mutation in the tumor positively influenced TDO2 but not IDO1 expression (4). In the same publication we reported that treatment of leiomyoma smooth muscle cells and myometrial smooth muscle cells spheroids with the TDO2 inhibitor, 680C91 but not the IDO1 inhibitor, Epacodostat significantly repressed cell proliferation and the expression of collagen types I and type III in a dose-dependent manner; these effects were more pronounced in leiomyoma smooth muscle cells spheroids compared with myometrial smooth muscle cells spheroids. These results suggested that TDO2 is the enzyme with greater significance than IDO1 in fibroid pathogenesis. In a subsequent publication we reported that fibroids are characterized by dysregulation of a number of other enzymes in the tryptophan degradation pathway, with overexpression of tryptophan hydroxylase 1, potassium channel in arabidopsis thaliana 2, solute carrier family 7 member 8, and solute carrier family 7 member 5 mRNA and reduced expression of kynureninase, tryptophanyl-tRNA synthetase 1 mRNA and no changes in the expression of tryptophanyl-tRNA synthetase 2, mitochondrial, arylformamidase, kynurenine 3-monooxygenase, and kynurenine aminotransferase 1, kynurenine aminotransferase III, and kynurenine aminotransferase IV compared with matched myometrium (5). Because kynurenine is a ligand of aryl hydrocarbon receptor (AhR) we measured the expression of CYP1B1, a marker of AhR activation and showed these levels to be higher in fibroids compared with myometrium (5). Another group also has reported on overexpression of TDO2 in fibroids (7). Based on our published in vitro data with compound 680C91 a specific TDO2 inhibitor on fibroid extracellular matrix (ECM) components and cellular proliferation we hypothesized that inhibition of TDO2 in vivo will have beneficial therapeutic effects for fibroids by reducing collagen expression and inhibiting cell proliferation, thereby causing shrinkage of tumors. To test this hypothesis, we used a mouse model for fibroids in which severe combined immunodeficiency (SCID) mice bearing human fibroid xenografts were treated with compound 680C91 or vehicle for 2 months.

MATERIALS AND METHODS

Fibroid Specimens Collection

To reduce the variance among fibroids, tumors between 2 and 5 cm in diameter and with intramural location ($n = 12$) were obtained from premenopausal patients undergoing hysterectomy for symptomatic fibroids at the Harbor-UCLA Medical Center. Endometrial hyperplasia and cancer were exclusionary criteria. Prior approval from the institutional review board (18CR-31752-01R) at the Lundquist Institute was obtained. Informed consent was obtained from all the patients participating in the study who were not taking any hormonal medications for at least 3 months preoperatively. The fresh tissues were used for cell isolation and for xenografts in the animal model, and the remaining tissues were snap-frozen and stored in liquid nitrogen for further analysis as described previously (8, 9).

Fibroid Animal Model

The protocol (32133-01) was approved by the institutional animal care and use committee at the Lundquist Institute at the Harbor-UCLA Medical Center. Female ovariectomized SCID/beige mice (Charles River Laboratories, Hollister, CA) 9–12 weeks old were implanted with pellets (Innovative Research of America, Sarasota, FL) containing estradiol (0.075 mg/60 d release) and progesterone (75 mg/60 d release) as reported previously (10, 11). A portion of fresh fibroid weighing 0.5 g was cut aseptically into 5–10 pieces using a razor blade and implanted in the flank of a mouse. A total of 12 pairs of explants were implanted in 24 mice with half receiving 680C91 and the other 12 mice receiving the vehicle, thus allowing comparison of each treated tumor to its own control. After 3 days of recovery, mice were injected daily with the vehicle or 680C91 (10 mg/Kg). The dose of 680C91 used was on the basis of a prior publication examining its efficacy in a mouse model of chronic asthma (12). 680C91 (Cayman Chemical, Ann Arbor, MI) was dissolved with DMSO (0.05 mg/ μ L), then diluted with a vehicle buffer (DMSO:saline=1:1:9) for intraperitoneal (i.p.) administration (total injection of 100 μ L volume per mouse). After 2 months of treatment animals were killed, and blood was obtained by cardiac puncture. Tumor explants were carefully dissected free of surrounding tissue and then were weighed and frozen. Animals were weighed before and after treatment with 680C91 or the vehicle.

Blood Chemistry Panel

We analyzed plasma chemistry after 8 weeks of treatment with the vehicle or 680C91. The plasma (100 μ L) was pipetted into the Comprehensive Diagnostic Profile Rotor (#500-1038; Abaxis, Union City, CA), and the values of glucose, creatinine, blood urea nitrogen, phosphorus, sodium, albumin, alkaline phosphatase, serum glutamic pyruvic transaminase, total protein, globulin, total bilirubin, and amylase were analyzed using the VetScan VS2 chemistry analyzer (Abaxis, Union City, CA).

Quantitative Reverse Transcription-Polymerase Chain Reaction

Total RNA was extracted from the xenografts using TRIzol (Thermo Fisher Scientific Inc., Waltham, MA). RNA

concentration and integrity were determined using a Nanodrop 2000c spectrophotometer (Thermo Scientific, Wilmington, DE) and an Agilent 2100 Bioanalyzer (Agilent Technologies, Santa Clara, CA) as described previously (13). Briefly, 2 μ g of RNA was reverse transcribed using random primers for selected genes according to the manufacturer's guidelines (Applied Biosystems, Carlsbad, CA). Quantitative reverse transcription-polymerase chain reaction was performed using the SYBR gene expression master mix (Applied Biosystems). Reactions were incubated for 10 minutes at 95°C followed by 40 cycles for 15 seconds at 95°C and 1 minute at 60°C. The expression levels of selected genes were quantified using Invitrogen StepOne System, with FBXW2 (F-box and WD repeat domain containing 2) used for normalization (14). All reactions were run in triplicate, and relative mRNA expression was determined using the comparative cycle threshold method ($2^{-\Delta\Delta Ct}$), as recommended by the supplier (Applied Biosystems). Values were expressed as fold change compared with the control group. The primer sequences used were as follows: CYP1B1 (sense 5'-GGCCACTACTGACATCTTC-3', antisense 5'-CGAGTCTGCATCAGGATAC-3'); FN1 (sense 5'-ACCGAAATCACAGCCAGTAG-3', antisense 5'-CCTCCTCACTCAGCTCATATTC-3'); CDK2 (sense, 5'-TTCCCTCATCAAGAGCTATCTGT-3'; antisense, 5'-ACCCGATGAGAATGGCAGAA-3'); E2F1 (sense 5'-GGACTCTTCGGAGAAGTTTCAGATC-3', antisense 5'-GGGCACAGGAAAAATCGA-3'); TGF- β 3 (sense 5'-CGGGCTTTGGACACCAATTA-3', antisense 5'-GGGCGCACAGCAGTTC-3'); IL8 (sense, 5'-CTTGGCAGCCTTCTGATTT-3'; antisense, 5'-TTCTTTAGACTCCTTGGCAAAA-3'); SPARC (sense, 5'-TACATCGGGCCTTGCAAATA-3'; antisense, 5'-TGTCTCATCCCTCTCATACA-3'); and FBXW2 (sense 5'-CCTCGTCTCTAAACAGTGAATAA-3', antisense 5'-GCGTCTGAACAGAATCATCTA-3').

Immunoblotting

The total protein isolated from xenografts of the vehicle and 680C91 groups was subjected to immunoblotting as described previously (15, 16). Briefly, samples were suspended in a radio-immunoprecipitation assay buffer containing 1 mM ethylenediamine tetra acetic acid and ethylene glycol tetra acetic acid (Boston BioProducts, Milford, MA) supplemented with 1 mM phenylmethylsulfonyl fluoride and a complete protease inhibitor mixture (Roche Diagnostics, Indianapolis, IN), sonicated, and centrifuged at 4°C for 10 minutes at 14,000 rpm. The concentration of protein was determined using the BCA Protein Assay Kit (Thermo Scientific Pierce, Waltham, MA). Equal aliquots (30 micrograms) of total protein for each sample were denatured with sodium dodecyl sulfate-polyacrylamide gel electrophoresis sample buffer and separated by electrophoresis on a sodium dodecyl sulfate-polyacrylamide gel. After transferring the samples to a nitrocellulose membrane, the membrane was blocked with TBS-Tween + 5% milk and probed with the following primary antibodies: CYP1B1, FN1, and SPARC (Proteintech Group, Inc., Chicago, IL). The membranes were washed with TBS containing 0.1% Tween-20 wash buffer after each antibody incubation cycle. SuperSignal West Pico Chemiluminescent Substrate (Thermo Scientific Pierce, Wal-

tham, MA) was used for detection, and photographic emulsion was used to identify the protein bands, which subsequently were quantified by densitometry. The densities of the specific protein bands were determined using the image J program (available at: <http://imagej.nih.gov/ij/>), normalized to a band obtained from staining the membrane with Ponceau S. Results were expressed as means \pm SEM as a ratio relative to the control group, designated as 1.

Measurement of Kynurenine

Kynurenine concentration in paired leiomyoma and myometrium homogenates ($n = 12$) was measured in duplicate using the Human Kynurenine ELISA kit (MBS766153; MyBioSource) according to the manufacturer's instructions. Absorbance of each plate was measured spectrophotometrically at a wavelength of 450 nm and the concentration was determined by comparing the optical density value of samples to the standard curve.

Enzyme-Linked Immunosorbent Assay

The total collagen content in xenografts of vehicle and 680C91 treated groups ($n = 12$) was measured in duplicate using the QuickZyme Total Collagen Assay Kit (QuickZyme Biosciences, Leiden, Netherlands) according to the manufacturer's instructions. The absorbance of each plate was measured spectrophotometrically at a wavelength of 570 nm, and the concentration was determined by comparing the optical density value of samples with the standard curve. The level of total collagens was calculated as μ g/ml of protein and reported as fold change compared with the vehicle group.

Immunohistochemistry

For immunohistochemistry, the xenografts were fixed with 4% paraformaldehyde in phosphate-buffered saline (PBS) and subsequently transferred to PBS containing 30% sucrose (wt/vol) until equilibrated in cold (4 °C). After fixation, 5 μ m-thick paraffin sections were treated three times with HistoClear (National Diagnostics, Atlanta, GA) for 5 minutes, rehydrated by a sequential ethanol wash, and then incubated in a target-retrieval solution (Dako, Carpinteria, CA, USA) in a microwave for 10 min to retrieve the antigens. For blocking, tissues were incubated for 10 minutes with a 3% solution of H₂O₂ followed by incubation with PBS-5% normal goat serum-0.2% Triton X-100. Tissue sections were incubated with primary antibody rabbit anti-Ki67 (dilution 1:250, 27309-1-AP; Proteintech Group, Inc, Rosemont, IL), rabbit anti-cleaved caspase-3 (dilution 1:50, #9664; Cell Signaling Technology, Danvers, MA), and mouse anti-E2F1 (dilution 1:50, sc-251; Santa Cruz Biotechnology, Inc., Dallas, TX) overnight at 4°C in a humidified chamber. The antigens then were visualized using biotinylated antibodies and streptavidin, conjugated with horseradish peroxidase. Control sections were incubated with the secondary antibody, with replacement of the primary antibody with the dilution reagent (Dako). Diaminobenzidine (Dako) served as the substrate. All sections were counterstained with hematoxylin and eosin. Immunostained sections were examined under a microscope

(Olympus IX83; Olympus Surgical Technologies America, San Jose, CA), and 5 representative images of each slide were analyzed quantitatively with the use of Halo software (Indica Labs Inc., Albuquerque, NM) and were averaged for comparative analysis between vehicle and 680C91 treatment groups in a blinded fashion.

Fibroid Explant Culture

Equal weights of fibroid explants (4–5-mm³ cubes) cut aseptically from the same patient were plated in 6-well in complete medium and incubated for 48 hours with tryptophan (0.8 mM) or tryptophan plus AhR antagonist (CH-223191; 10 μ M) or TDO2 inhibitor (680C91; 50 μ M).

Statistics and Power Analysis

Throughout the text, results are presented as mean \pm SEM and data were analyzed by GraphPad PRISM 10 software (GraphPad, San Diego, CA). Data set normality was determined by the Kolmogorov–Smirnov test. The data presented in this study were not normally distributed, and therefore nonparametric tests were used for data analysis. Comparisons involving 2 groups were analyzed using the Wilcoxon matched pairs signed rank test as appropriate. The Kruskal–Wallis test was used for comparisons involving multiple groups. The relationship between two expression groups was determined using the Spearman r correlation coefficient. Statistical significance was established at $P < .05$.

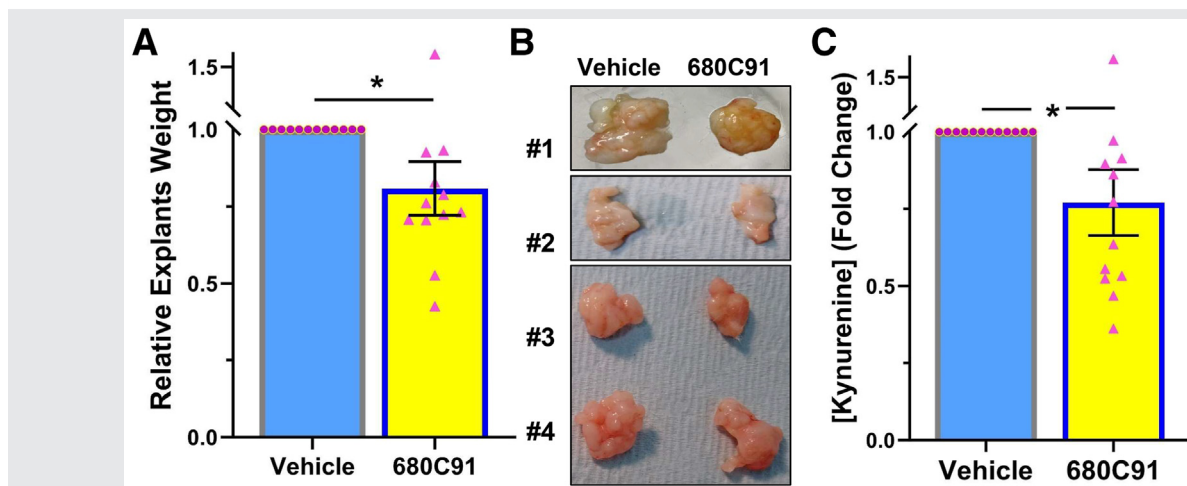
RESULTS

The administration of 680C91 was well-tolerated. [Supplementary Table 1](#) (available online) shows the results of

blood chemistry after 2 months of treatment with the drug. There were no effects of 680C91 on liver, kidney or pancreatic function and no effects on body weight of the animals.

There was an approximately 30% reduction in the weight of fibroid explants in mice treated with 680C91 ([Fig. 1A](#)). Representative images of fibroid xenografts treated with vehicle or 680C91 are shown in [Fig. 1B](#). As expected, there was a reduction in kynurenine levels ([Fig. 1C](#)) in the xenografts from animals treated with 680C91 compared with vehicle-treated mice, which indicates that the drug effectively inhibited TDO2 enzyme activity. The xenografts were analyzed for a number of key genes known to have a role in fibroid pathogenesis. As shown in [Fig. 2A](#) treatment with the inhibitor resulted in decreased mRNA expression of the profibrotic cytokine transforming growth factor β 3 (TGF- β 3) (17–19), the inflammatory gene marker interleukin-8 (IL-8) (20), the cell cycle regulatory genes (*E2F1* and *CDK2*) (17, 21), FN1, a major component of the ECM (22) and SPARC, a matricellular protein involved in ECM remodeling and composition (23). Treatment with 680C91 also inhibited the expression of *CYP1B1*, a gene regulated by AhR and a marker for its activation (24). We also measured total collagen protein levels in the xenografts and as shown in [Figure 2B](#) there was a significant decrease in total collagen protein levels in xenografts of mice treated with 680C91. The levels of *CYP1B1*, FN1, and SPARC also were measured by Western blot analysis and in concordance with the mRNA expression there was decreased protein abundance in the xenografts of mice treated with 680C91 compared with vehicle-treated mice ([Fig. 2C](#) and [D](#)). We did not find significant effect of the inhibitor on TGF- β 3, IL-8, and CDK2 at the protein levels as determined by enzyme-linked immunosorbent assay and Western blot analysis (data not shown).

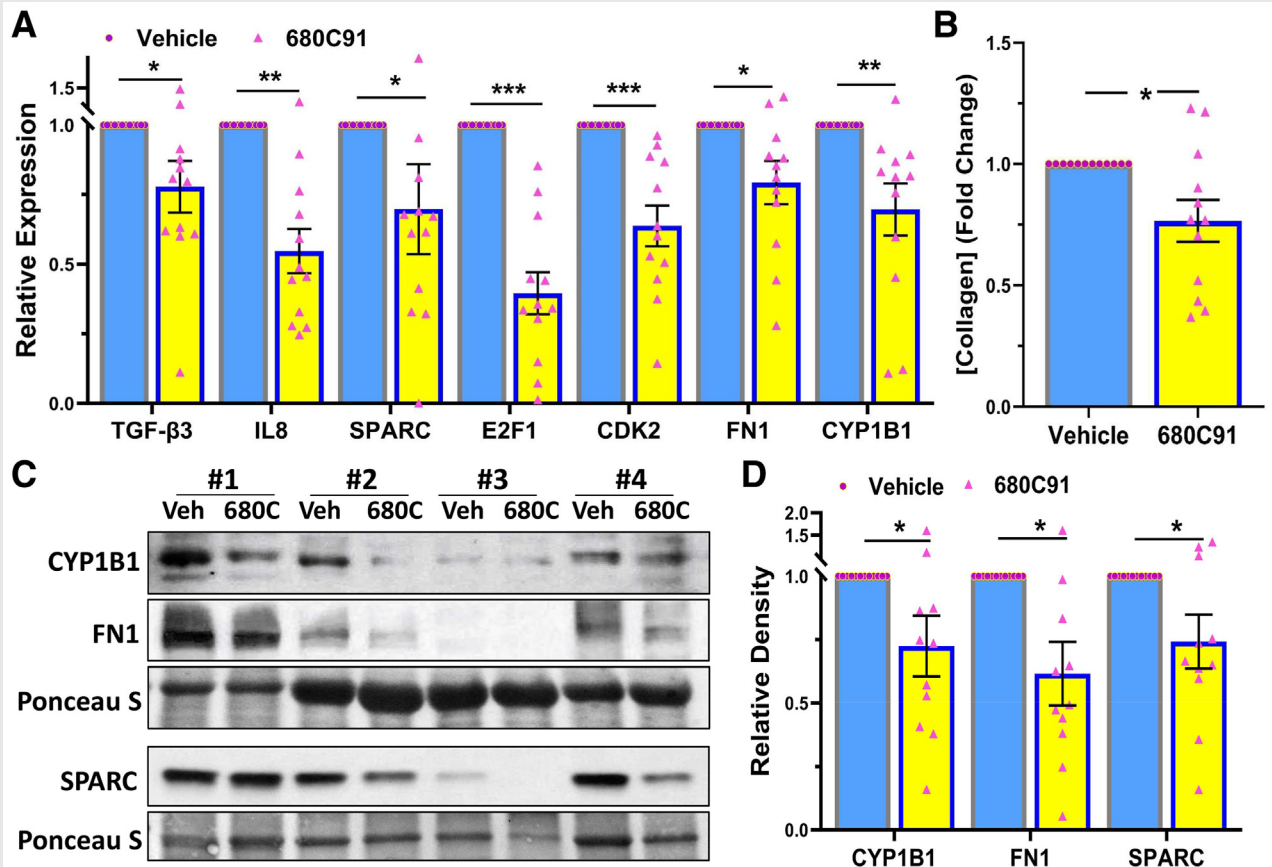
FIGURE 1



(A) Fresh fibroid explants were implanted subcutaneously in the flank of ovariectomized CB-17 SCID/Beige mice and treated intraperitoneally daily for 2 months with the vehicle or TDO2 inhibitor (680C91; 10 mg/Kg). The weight of tumor explants was determined after 8 weeks of treatment ($n = 12$). (B) Representative images of 4 xenografts at the end of treatment period (8 weeks). (C) Kynurenine levels as determined by enzyme-linked immunosorbent assay in 12 xenografts. The results are presented as mean \pm SEM of independent experiments with P values indicated at the corresponding line. * $P < .05$.

Chuang. Effect of 680c91 in a fibroid mouse model. *Fertil Steril* 2024.

FIGURE 2



(A) Relative mRNA expression of FN1, CYP1B1, E2F1, CDK2, TGF- β 3, IL8 and SPARC in (A) xenografts implanted subcutaneously in the ovariectomized CB-17 SCID/Beige mice ($n = 12$) after 8 weeks of treatment with vehicle or TDO2 inhibitor (680C91; 10 mg/Kg). (B) Total collagen levels as determined by enzyme-linked immunosorbent assay in 12 xenografts. (C) Representative Western blot analysis of CYP1B1, FN1 and SPARC with bar graphs (D) showing their relative band densities in the xenografts ($n = 12$). The results are presented as mean \pm SEM of independent experiments with P values indicated at the corresponding line. * $P < .05$; ** $P < .01$; *** $P < .001$.

Chuang. Effect of 680C91 in a fibroid mouse model. *Fertil Steril* 2024.

The xenografts also were subjected to histologic and immunohistochemical staining and image analysis using Halo software (Fig. 3). As shown in Figure 3A and B, staining of xenograft section with Masson's trichrome stain showed that explants from the 680C91-treated mice had significantly reduced staining for collagen as indicated by the blue stain. These xenografts also showed a significant decrease in cell proliferation as indicated by the reduced nuclear staining for Ki67 (Fig. 3C and D), but no significant change in apoptosis as indicated by cleaved caspase 3 staining (Fig. 3E and F). There also was a significant reduction in staining for E2F1, a cell cycle regulatory protein (Fig. 3G and H) consistent with the mRNA expression.

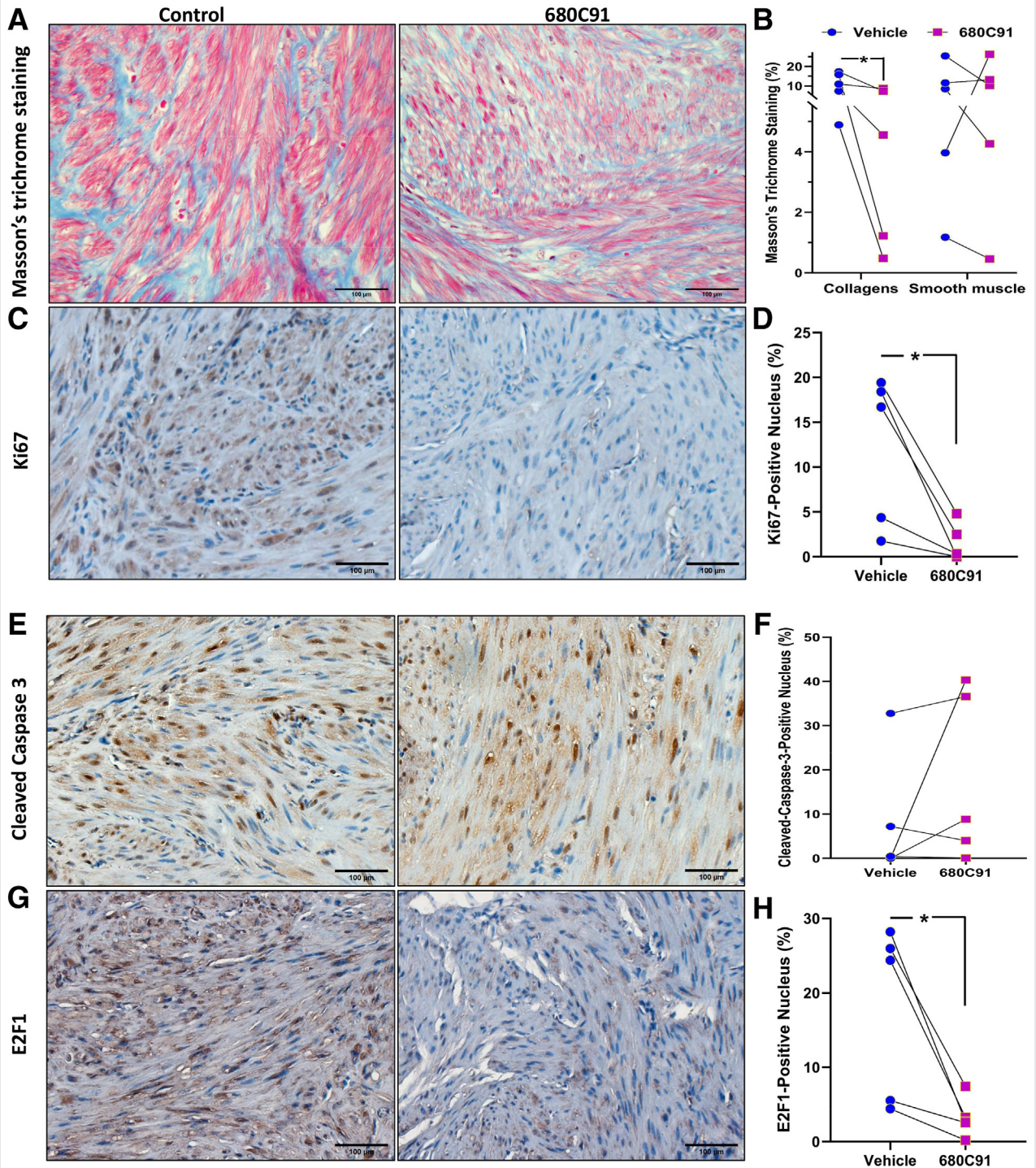
We performed correlation analysis between the levels of kynurenine in the xenografts and various parameters including tumor weight (Fig. 1A) and FN1 levels (Fig. 2). As shown in Figure 4A and B there is a significant direct correlation between the xenograft kynurenine levels and tumor weight and FN1 protein. We also detected a significant correlation between the tumor weight and FN1 mRNA (Fig. 4C).

To determine the mechanism by which the TDO2 inhibitor exerts its effects in vitro studies were carried out with fibroid explants treated with tryptophan alone and tryptophan plus the 680C91 and the AhR antagonist CH-223191. After 48 hours of culture the explants were analyzed for the expression of the same genes (Fig. 2) we found to be altered significantly by in vivo administration of 680C91. As shown in Figure 4D, tryptophan significantly induced the expression of TGF- β 3, SPARC, IL-8, E2F1, CDK2, FN1, and CYP1B1 mRNA. The effects of tryptophan were blocked by cotreatment with the TDO2 inhibitor 680C91 and by the AhR antagonist CH-223191 indicating that the observed in vivo effects of 680C91 are mediated by AhR pathway.

DISCUSSION

The results of this preclinical study indicate that treatment of mice bearing human fibroid xenografts with compound 680C91, a specific inhibitor of TDO2, results in 30% reduction in tumor weight after 2 months of treatment. In response to

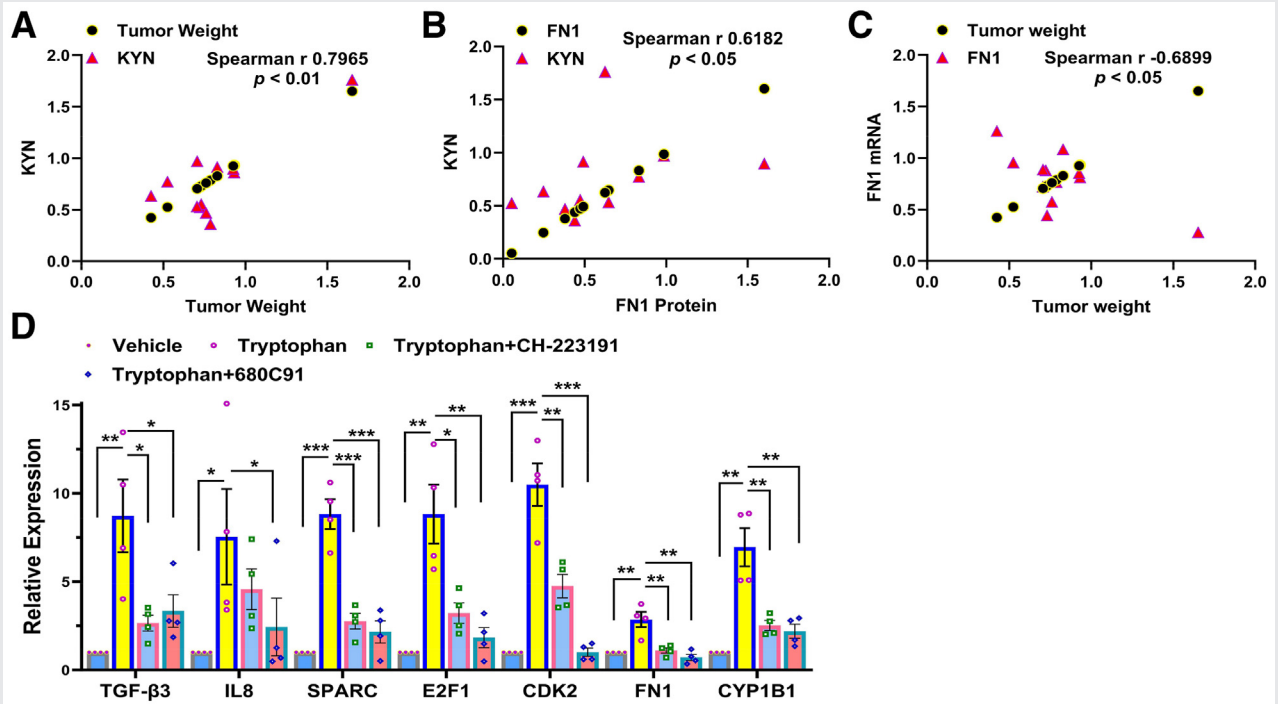
FIGURE 3



(A, B) Representative histopathologic images determined by Masson's trichrome staining of fibroid xenografts from vehicle or TDO2 inhibitor-treated group. Blue color demonstrates collagen fibers and red color indicates smooth muscle cells. (B) Shows the quantification of staining intensity by Halo software. (C-H) Representative immunohistochemical stained images of fibroid xenografts treated with vehicle or TDO2 inhibitor for Ki67 (C, D), Cleaved Caspase 3 (E, F), and E2F1 (G, H). Image analysis of nuclear staining was done by Halo software. The results are presented as mean ± SEM with P values indicated at the corresponding line. *P<.05.

Chuang. Effect of 680c91 in a fibroid mouse model. *Fertil Steril* 2024.

FIGURE 4



Correlation analysis between the fold change in (A) tumor weight with kynurenine level in the xenografts, (B) xenograft kynurenine level with FN1 protein, and (C) tumor weight with FN1 mRNA level in the xenografts (D). Fibroid explants ($n = 3$) were treated with tryptophan (0.8 mM) or tryptophan plus AhR antagonist (CH-223191; 10 μ M) or TDO2 inhibitor (680C91; 50 μ M) for 48 hours and mRNA expression was determined by real time polymerase chain reaction. The results are presented as mean \pm SEM with P values indicated by corresponding lines. * $P < .05$; ** $P < .01$; *** $P < .001$.

Chuang. Effect of 680c91 in a fibroid mouse model. *Fertil Steril* 2024.

the inhibitor treatment, there was a significant reduction in kynurenine levels in the xenografts indicating efficient inhibition of TDO2 to break down tryptophan to kynurenine. Furthermore, we found a direct correlation between kynurenine levels in the xenografts and the decrease in fibroid weight and the expression of FN1, a major component of the ECM. Gene profiling of the xenografts from the compound 680C91-treated mice compared with matched xenografts from vehicle-treated mice revealed a significant reduction in TGF- β 3, FN1, CDK2, E2F1, IL-8, SPARC, and CYP1B1 mRNA expression. These xenografts also expressed lower total collagen, FN1, and CYP1B1 protein levels compared with vehicle-treated animals. Immunohistochemical and histologic analysis of xenografts indicated a decreased expression of collagen, Ki67, E2F1 in mice treated with the inhibitor. In vitro studies with fibroid explants treated with tryptophan indicated an induction of TGF- β 3, FN1, CDK2, E2F1, IL-8, SPARC, and CYP1B1 mRNA and this induction could be blocked by 680C91 and the AhR antagonist CH-223191 indicating that the observed in vivo effects of 680C91 are mediated by the AhR pathway. The promising results from this preclinical in vivo study with the inhibitor of TDO2 indicate that correction of markedly dysregulated degradation of tryptophan demonstrated previously by our group (4, 5) could be an effective therapy for fibroids.

The degradation of tryptophan by TDO2 results in production of kynurenine, which is a ligand for AhR, a transcription factor and member of the basic helix-loop-helix/Per-ARNT-SIM (bHLH-PAS) family (25). Our results indicate that inhibition of TDO2 results in downregulation of *CYP1B1*, which is a downstream gene regulated by AhR. After binding of AhR to its ligand it dimerizes with AhR nuclear translocator (ARNT) and acts as a transcription factor affecting transcription of wide array of genes that bear the xenobiotic response element (25). The AhR signaling is involved in diverse processes many of which are relevant to fibroid pathophysiology. AhR signaling stimulates oxidative stress (26), inhibits autophagy (27–29) and is involved in the inflammatory process although its interaction with NF- κ B (30, 31). This signaling pathway also is involved in the differentiation of immune cells by enhancing the generation of immunosuppressive phenotype (31).

Our data indicate that the decrease in the weight of fibroid explants in response to TDO2 inhibitor treatment is primarily due to the drug effect on cell proliferation and not cellular apoptosis. This decrease in cell proliferation is evidenced by decreased Ki67 expression in xenograft from animals treated with 680C91, and decreased expression of genes critical in cell cycle regulation namely CDK2, a serine/threonine protein kinase which regulates G1/S phase transition (32), and E2F1 a

transcription factor which has a critical role in the control of cell cycle and apoptosis (33). Both E2F1 and CDK2 are overexpressed in fibroids (17, 21). E2F1 also directly interacts with AhR displacing p300 protein from the complex resulting in the inhibition of transcription of many E2F regulated genes that control the S phase progression (34). The interaction between E2F and AhR also was shown to lead to inhibition of E2F1-induced apoptosis in mouse hepatoma cells and human osteosarcoma cells (35). In addition to its inhibitory effects on cell proliferation, the reduction in fibroid xenografts weight following the TDO2 inhibitor treatment could be secondary to a reduction in ECM volume as evidenced by decreased expression of collagens and FN1, and the direct correlation between FN1 levels, a major component of the ECM and tumor weight.

A hallmark of fibroids is the accumulation of ECM with overexpression of collagen and fibronectin (1–3). Additionally, these tumors overexpress TGF- β 3 which is a master regulator of fibrosis (17–19). Compound 680C91 inhibited the expression of TGF- β 3 mRNA and the expression of collagens and FN1 protein in the fibroid xenografts. Some of these effects could be secondary to the inhibition of AhR signaling as evidenced by decreased CYP1B1 levels in the xenografts of the inhibitor-treated mice, and our in vitro data showing blockade of tryptophan induction of TGF- β 3 and FN1 by the AhR antagonist. The TDO2 inhibitor also inhibited the expression of SPARC in vivo, and our in vitro finding indicated that this effect is mediated by AhR. Recently our group reported a marked overexpression of SPARC in fibroids compared with their matched myometrium (36). The SPARC is a matricellular secreted glycoprotein that directly binds to the ECM collagen and activates MMPs (37, 38) and indirectly regulates growth factors involved in angiogenesis and tissue remodeling including FGF, VEGF, and TGF- β (23). Also AhR signaling is known to interact with the NF- κ B pathway (30, 31, 39) and TGF signaling pathway (40) both pathways having critical roles in fibroid pathogenesis (1–3).

Another mechanism by which 680C91 can exert its effects could be immune mediated. Activation of AhR by kynurenine dampens the immune response to prevent excessive inflammation and autoimmunity by production of excess amounts of immunosuppressive metabolites of the kynurenine pathway (41). The metabolites of the kynurenine degradation pathway have an immunosuppressive role due to their ability to suppress T cell reactivity and represents a mechanism by which tumors escape an immune response. Multiple clinical trials are underway to examine the efficacy of TDO2/IDO1 inhibitors with the goal to reduce kynurenine and other immunosuppressive tryptophan catabolites, thereby reverting the immunosuppressive microenvironment induced by tryptophan catabolites. These drugs, which resemble tryptophan (also referred to as checkpoint inhibitors), have shown promise for cancer immunotherapy (42). Because these drugs mimic tryptophan, they can have off target effects and can activate the AhR. The activation of AhR could have procarcinogenic effects in some human cancers, such as lung, prostate, breast, and pancreatic cancer, whereas in other cancers, such as colon cancer, it could

have anticarcinogenic effect (43). In this study, 680C91 did not have an activation effect on AhR. The activation of AhR by kynurenine also has epigenetic effects that could lead to chromatin remodeling. The AhR-ARNT interacts with several histone acetyltransferases and chromatin remodeling factors to block histone acetylation (44).

In summary, our data indicate that inhibition of TDO2 expression by 680C91 has beneficial effects by reducing fibroid growth through its inhibitory effect on cell proliferation. In addition, the inhibitor treatment induced a favorable gene profile in the fibroid with a reduction in the ECM volume as indicated by decreased collagens and FN1 expression, reduced inflammation as indicated by decreased expression of inflammatory genes, SPARC, and IL-8, and decreased fibrosis as indicated by reduced TGF- β 3 expression in the tumors. The effects of compound 680C91 are most likely due to its effect to reduce kynurenine production and thereby decreased AhR activation as evidenced by our findings of lower CYP1B1 mRNA/protein in fibroid xenografts and our in vitro experiments with fibroid explants. These promising therapeutic effects of TDO2 inhibitor for the treatment of fibroids warrant additional animal studies and phase 1 human clinical trial.

CRediT Authorship Contribution Statement

Tsai-Der Chuang: Conceptualization, Data curation, Formal analysis, Investigation, Methodology, Project administration, Writing – original draft, Writing – review & editing. **Nhu Ton:** Data curation, Investigation. **Shawn Rysling:** Data curation, Investigation. **Derek Quintanilla:** Data curation, Investigation. **Drake Boos:** Data curation, Investigation. **Omid Khorram:** Conceptualization, Funding acquisition, Investigation, Methodology, Project administration, Resources, Supervision, Writing – original draft, Writing – review & editing, Formal analysis.

Declaration of Interests

T.D.C. and O.K. report a patent “Use of Tryptophan 2,3 dioxygenase (TDO2) inhibitors for treatment of fibroids” was applied in 2021. N.T. has nothing to disclose. S.R. has nothing to disclose. D.K. has nothing to disclose. D.B. has nothing to disclose.

REFERENCES

- Segars JH, Parrott EC, Nagel JD, Guo XC, Gao X, Birnbaum LS, et al. Proceedings from the Third National Institutes of Health International Congress on Advances in Uterine Leiomyoma Research: comprehensive review, conference summary and future recommendations. *Hum Reprod Update* 2014; 20:309–33.
- Stewart EA, Laughlin-Tommaso SK, Catherino WH, Lalitkumar S, Gupta D, Vollenhoven B. Uterine fibroids. *Nat Rev Dis Primers* 2016;2:16043.
- Stewart EA, Cookson CL, Gandolfo RA, Schulze-Rath R. Epidemiology of uterine fibroids: a systematic review. *BJOG* 2017;124:1501–12.
- Chuang TD, Quintanilla D, Boos D, Khorram O. Tryptophan catabolism is dysregulated in leiomyomas. *Fertil Steril* 2021;116:1160–71.
- Chuang TD, Quintanilla D, Boos D, Khorram O. Further characterization of tryptophan metabolism and its dysregulation in fibroids. *F S Sci* 2022;3: 392–400.

6. Cheong JE, Sun L. Targeting the IDO1/TDO2-KYN-AhR Pathway for cancer immunotherapy – challenges and opportunities. *Trends Pharmacol Sci* 2018;39:307–25.
7. Hutchinson AP, Yin P, Neale I, Coon JSt, Kujawa SA, Liu S, et al. Tryptophan 2,3-dioxygenase-2 in uterine leiomyoma: dysregulation by MED12 mutation status. *Reprod Sci* 2022;29:743–9.
8. Chuang TD, Ton N, Rysling S, Quintanilla D, Boos D, Gao J, et al. The influence of race/ethnicity on the transcriptomic landscape of uterine fibroids. *Int J Mol Sci* 2023;24.
9. Chuang TD, Munoz L, Quintanilla D, Boos D, Khorram O. Therapeutic effects of long-term administration of tranilast in an animal model for the treatment of fibroids. *Int J Mol Sci* 2023;24.
10. Ishikawa H, Ishi K, Serna VA, Kakazu R, Bulun SE, Kurita T. Progesterone is essential for maintenance and growth of uterine leiomyoma. *Endocrinology* 2010;151:2433–42.
11. Ono M, Yin P, Navarro A, Moravek MB, Coon JSt, Druschitz SA, et al. Paracrine activation of WNT/beta-catenin pathway in uterine leiomyoma stem cells promotes tumor growth. *Proc Natl Acad Sci U S A* 2013;110:17053–8.
12. Cuartero MI, Ballesteros I, de la Parra J, Harkin AL, Abautret-Daly A, Sherwin E, et al. L-kynurenine/aryl hydrocarbon receptor pathway mediates brain damage after experimental stroke. *Circulation* 2014;130:2040–51.
13. Chuang TD, Gao J, Quintanilla D, McSwiggin H, Boos D, Yan W, et al. Differential expression of MED12-associated coding RNA transcripts in uterine leiomyomas. *Int J Mol Sci* 2023;24:3742.
14. Almeida TA, Quispe-Ricalde A, Montes de Oca F, Foronda P, Hernandez MM. A high-throughput open-array qPCR gene panel to identify housekeeping genes suitable for myometrium and leiomyoma expression analysis. *Gynecol Oncol* 2014;134:138–43.
15. Chuang TD, Rehan A, Khorram O. Functional role of the long noncoding RNA X-inactive specific transcript in leiomyoma pathogenesis. *Fertil Steril* 2021;115:238–47.
16. Chuang TD, Rehan A, Khorram O. Tranilast induces miR-200c expression through blockade of RelA/p65 activity in leiomyoma smooth muscle cells. *Fertil Steril* 2020;113:1308–18.
17. Chuang TD, Khorram O. Tranilast inhibits genes functionally involved in cell proliferation, fibrosis, and epigenetic regulation and epigenetically induces miR-29c expression in leiomyoma cells. *Reprod Sci* 2017;24:1253–63.
18. Chuang TD, Khorram O. Cross-talk between miR-29c and transforming growth factor- β 3 is mediated by an epigenetic mechanism in leiomyoma. *Fertil Steril* 2019;112:1180–9.
19. Chuang TD, Quintanilla D, Boos D, Khorram O. Long noncoding RNA MIAT modulates the extracellular matrix deposition in leiomyomas by sponging miR-29 family. *Endocrinology* 2021;162:bqab186.
20. Kany S, Vollrath JT, Relja B. Cytokines in inflammatory disease. *Int J Mol Sci* 2019;20.
21. Chuang TD, Khorram O. Regulation of cell cycle regulatory proteins by microRNAs in uterine leiomyoma. *Reprod Sci* 2019;26:250–8.
22. Dalton CJ, Lemmon CA. Fibronectin: molecular structure, fibrillar structure and mechanochemical signaling. *Cells* 2021;10.
23. Arnold SA, Brekken RA. SPARC: a matricellular regulator of tumorigenesis. *J Cell Commun Signal* 2009;3:255–73.
24. Tsuchiya Y, Nakajima M, Yokoi T. Critical enhancer region to which AhR/ARNT and Sp1 bind in the human CYP1B1 gene. *J Biochem* 2003;133:583–92.
25. Kolonko M, Greb-Markiewicz B. bHLH-PAS Proteins: their structure and intrinsic disorder. *Int J Mol Sci* 2019;20.
26. Furue M. Regulation of Skin barrier function via competition between AHR axis versus IL-13/IL-4–JAK–STAT6/STAT3 axis: pathogenic and therapeutic implications in atopic dermatitis. *J Clin Med* 2020;9.
27. Peng G, Tsukamoto S, Ikutama R, Nguyen HLT, Umehara Y, Trujillo-Paez JV, et al. Human β -defensin-3 attenuates atopic dermatitis-like inflammation through autophagy activation and the aryl hydrocarbon receptor signaling pathway. *J Clin Invest* 2022;132.
28. Wnuk A, Rzemieniec J, Przepiórska K, Wesolowska J, Wójtowicz AK, Kajta M. Autophagy-related neurotoxicity is mediated via AHR and CAR in mouse neurons exposed to DDE. *Sci Total Environ* 2020;742:140599.
29. Miao Y, Lv Q, Qiao S, Yang L, Tao Y, Yan W, et al. Alpinetin improves intestinal barrier homeostasis via regulating AhR/suv39h1/TSC2/mTORC1/autophagy pathway. *Toxicol Appl Pharmacol* 2019;384:114772.
30. Bankoti J, Rase B, Simones T, Shepherd DM. Functional and phenotypic effects of AhR activation in inflammatory dendritic cells. *Toxicol Appl Pharmacol* 2010;246:18–28.
31. Guarnieri T. Aryl hydrocarbon receptor connects inflammation to breast cancer. *Int J Mol Sci* 2020;21.
32. Fagundes R, Teixeira LK. Cyclin E/CDK2: DNA replication, replication stress and genomic instability. *Front Cell Dev Biol* 2021;9:774845.
33. Ertosun MG, Hapil FZ, Osman Nidai O. E2F1 transcription factor and its impact on growth factor and cytokine signaling. *Cytokine Growth Factor Rev* 2016;31:17–25.
34. Marlowe JL, Knudsen ES, Schwemberger S, Puga A. The aryl hydrocarbon receptor displaces p300 from E2F-dependent promoters and represses S phase-specific gene expression. *J Biol Chem* 2004;279:29013–22.
35. Marlowe JL, Fan Y, Chang X, Peng L, Knudsen ES, Xia Y, et al. The aryl hydrocarbon receptor binds to E2F1 and inhibits E2F1-induced apoptosis. *Mol Biol Cell* 2008;19:3263–71.
36. Chuang TD, Quintanilla D, Boos D, Khorram O. Differential expression of super-enhancer-associated long non-coding RNAs in uterine leiomyomas. *Reprod Sci* 2022;29:2960–76.
37. McClung HM, Thomas SL, Osenkowski P, Toth M, Menon P, Raz A, et al. SPARC upregulates MT1-MMP expression, MMP-2 activation, and the secretion and cleavage of galectin-3 in U87MG glioma cells. *Neurosci Lett* 2007;419:172–7.
38. Fujita T, Shiba H, Sakata M, Uchida Y, Nakamura S, Kurihara H. SPARC stimulates the synthesis of OPG/OCIF, MMP-2 and DNA in human periodontal ligament cells. *J Oral Pathol Med* 2002;31:345–52.
39. Celik-Turgut G, Olmez N, Koc T, Ozgun-Acar O, Semiz A, Dodurga Y, et al. Role of AHR, NF- κ B and CYP1A1 crosstalk with the X protein of hepatitis B virus in hepatocellular carcinoma cells. *Gene* 2023;853:147099.
40. Yang CE, Wang YN, Hua MR, Miao H, Zhao YY, Cao G. Aryl hydrocarbon receptor: from pathogenesis to therapeutic targets in aging-related tissue fibrosis. *Ageing Res Rev* 2022;79:101662.
41. Hubbard TD, Murray IA, Perdeu GH. Indole and tryptophan metabolism: endogenous and dietary routes to Ah receptor activation. *Drug Metab Dispos* 2015;43:1522–35.
42. Amobi A, Qian F, Lugade AA, Odunsi K. Tryptophan catabolism and cancer immunotherapy targeting IDO mediated immune suppression. *Adv Exp Med Biol* 2017;1036:129–44.
43. Günther J, Däbritz J, Wirthgen E. Limitations and off-target effects of tryptophan-related IDO inhibitors in cancer treatment. *Front Immunol* 2019;10:1801.
44. Schnekenburger M, Peng L, Puga A. HDAC1 bound to the Cyp1a1 promoter blocks histone acetylation associated with Ah receptor-mediated trans-activation. *Biochim Biophys Acta* 2007;1769:569–78.

Efectos terapéuticos del inhibidor de triptófano 2,3-dioxigenasa (680c91) para el tratamiento de fibromas: un estudio preclínico

Objetivo: Los fibromas se caracterizan por una marcada sobreexpresión de triptófano 2,3 dioxigenasa (TDO2). El objetivo de este estudio fue determinar la eficacia de la administración in vivo de un inhibidor de TDO2 (680C91) sobre el tamaño de los fibromas y la expresión génica.

Diseño: Estudio en animales y tejidos humanos ex vivo

Escenario: Institución de Investigación Académica

Sujetos: Ratones con inmunodeficiencia combinada grave portadores de xenoinjertos de fibromas humanos tratados con vehículo e inhibidor de TDO2

Intervención: Administración intraperitoneal diaria de 680C91 o vehículo por 2 meses y estudios in vitro con explantes de fibroma

Medición del resultado principal: Peso tumoral y perfil de expresión génica de xenoinjertos y experimentos mecánicos in vitro usando fibromas explantados

Resultados: El compuesto 680C91 fue bien tolerado sin efectos sobre la química sanguínea ni el peso corporal. El tratamiento de ratones con 680C91 resultó en una reducción del 30% en el peso de los xenoinjertos de fibromas después de 2 meses de tratamiento y, como se esperaba, niveles más bajos de quinurenina, el subproducto de la degradación del triptófano y un ligando endógeno del receptor de aril hidrocarburo (AhR) en los xenoinjertos. La expresión del citocromo P450 familia 1 subfamilia B miembro 1 (CYP1B1), factor de crecimiento transformante b3 (TGF-b3), fibronectina (FN1), quinasa ciclindependiente 2 (CDK2), factor de transcripción E2F 1 (E2F1), interleucina 8 (IL-8) y proteína secretada ácida y rica en cisteína (SPARC) fueron más bajas en los xenoinjertos de ratones tratados con 680C91 en comparación con los controles del vehículo. De manera similar, la proteína que abunda en el colágeno, FN1, CYP1B1 y SPARC fue menor en los xenoinjertos de ratones tratados con 680C91 en comparación con los controles. El análisis inmunohistoquímico de xenoinjertos indicó una disminución de la expresión de colágeno, Ki67 y E2F1, pero no cambios significativos en la expresión de caspasa 3 escindida en ratones tratados con 680C91. Los niveles de quinurenina en los xenoinjertos mostraron una correlación directa con el peso del tumor y los niveles de FN1. Los estudios in vitro con explantes de fibromas mostraron una inducción significativa de CYP1B1, ARNm de TGF-b3, FN1, CDK2, E2F1, IL8 y mARN SPARC por triptófano, que podría bloquearse mediante cotratamiento con 680C91 y el antagonista de AhR CH-223191.

Conclusión: Los resultados indican que la corrección del catabolismo aberrante del triptófano en fibromas puede ser un tratamiento efectivo a través del cual se reduzca la proliferación celular y la acumulación de matrix extracelular.